Non-harmonic potential of a single beam optical trap

A.C. Richardson[1,†], **S.N.S. Reihani**[1,2,†], **and L.B. Oddershede**[1*]

[1]*The Niels Bohr Institute, University of Copenhagen, Blegdamsvej 17, 2100 Copenhagen, Denmark.*

[2]*The Institute for Advanced Studies in Basic Sciences, P.O.Box:45195-1159, Zang, Zanjan, Iran.*

[†] *These authors contributed equally to this work.*

[*] *Corresponding author: oddershede@nbi.dk*

Abstract: Since the invention of optical traps based on a single laser beam, the potential experienced by a trapped specimen has been assumed harmonic, in the central part of the trap. It has remained unknown to what extent the harmonic region persists and what occurs beyond. By employing a new method, we have forced the trapped object to extreme positions, significantly further than previously achieved in a single laser beam, and thus experimentally explore an extended trapping potential. The potential stiffens considerably as the bead moves to extreme positions and therein is not well described by simple Uhlenbeck theories.

OCIS codes: (140.7010) Laser trapping; (170.4520) Optical confinement and manipulation; (350.4855) Optical tweezers or optical manipulation.

References and links

1. A. Ashkin, J. M. Dziedzic, J. E. Bjorkholm, and S. Chu, "Observation of a single-beam gradient force optical trap for dielectric particles," Opt. Lett. **11,** 288–290 (1986).
2. S. Kuo and M. Sheetz, "Force of single kinesin molecules measured with optical tweezers," Science **260,** 232–234 (1993).
3. K. Svoboda, C. Schmidt, B. Schnapp, and S. Block, "Direct observation of kinesin stepping by optical trapping interferometry," Nature (London) **365,** 721–727 (1993).
4. M. Wang, M. Schnitzer, H. Yin, and R. Landick, "Force and velocity measured for single molecules of RNA polymerase," Science **282,** 902–907 (1998).
5. I. Vladescu, M. McCauley, M. Nünez, I. Rouzina, and M. Williams, "Quantifying force-dependent and zero-force DNA intercalation by single-molecule stretching," Nature Methods **4,** 517–522 (2007).
6. A. Ashkin, "Forces of a single-beam gradient laser trap on a dielectric sphere in the ray optics regime," Biophys. J. **61,** 569–582 (1992).
7. Z. Gong, Z. Wang, Y. Li, L. Lou, and S. Xu, "Axial deviation of an optically trapped particle in trapping force calibration using the drag force method," Opt. Commun. **273,** 37–42 (2007).
8. A. Rohrbach, "Stiffness of optical traps: quantitative agreement between experiment and electromagnetic theory," Phys. Rev. Lett. **95,** 168102-1–168102-4 (2005).
9. C. Wang and G. Uhlenbeck, "Selected papers on noise and stochastic processes," (Dover, New York, 1952).
10. F. Gittes and C. Schmidt, "Signals and noise in micromechanical measurements," Methods in cell Biology **55,** 129–156 (1998).
11. K. Berg-Sørensen and H. Flyvbjerg, "Power spectrum analysis for optical tweezers," Rev. Sci. Instrum. **75,** 594–612 (2004).
12. F. Merenda, G. Boer, J. Rohner, G. Delacrétaz, and R. Salathé, "Escape trajectories of single-beam optically trapped micro-particles in a transverse fluid flow," Opt. Express **14,** 1685–1699 (2006), http://www.opticsexpress.org/abstract.cfm?uri=oe-14-4-1685.

#99368 - $15.00 USD Received 1 Aug 2008; revised 12 Sep 2008; accepted 15 Sep 2008; published 19 Sep 2008

13. E. Fällman and O. Axner, "Influence of a glass-water interface on the on-axis trapping of micrometer-sized spherical objects by optical tweezers," Appl. Opt. **42,** 3915–3926 (1993).
14. S. Reihani and L. Oddershede, "Optimizing immersion media refractive index improves optical trapping by compensating spherical aberrations," Opt. Lett. **32,** 1998–2000 (2007).
15. M. Speidel, A. Jonáš, and E. L. Florin, "Three-dimensional tracking of fluorescent nanoparticles with sub-nanometer precision by use of off-focus imaging," Opt. Lett. **28,** 69–71 (2003).
16. L. Oddershede, S. Grego, S. Nørrelykke, and K. Berg-Sørensen, "Optical tweezers: probing biological surfaces," Probe microscopy **2,** 129–137 (2001).
17. P. Hansen, I. Tolic-Nørrelykke, H. Flyvbjerg, and K. Berg-Sørensen, "tweezercalib 2.1: Faster version of MatLab package for precise calibration of optical tweezers," Comput. Phys. Commun. **174,** 572–573 (2006).
18. V. Bormuth, A. Jannash, M. Ander, C.M. van Kats, A. van Blaadern, J. Howard, and E. Schäffer, "Optical trapping of coated microspheres," Opt. Express **16,** 13831–13833 (2008).
19. A.A.R. Neves, A. Fontes, L.Y. Pozzo, A. Thomaz, E. Chillce, E.Rodriguez, L.C. Barbosa, and C.L. Cesar, "Electromagnetic forces for an arbitrary optical trapping of a spherical dielectric," Opt. Express **14,** 13101–13106 (2006).
20. T.A. Nieminen, V.L.Y. Loke, A.B. Stilgoe, G. Knöner, A.M. Branczyk, N.R. Heckenberg, and H. Rubinsztein-Dunlop, "Optical tweezers computational toolbox," J. Optic. Pure. Appl. Optic. **9,**, S196–S203 (2007).
21. F.G. Smith and T.A. King . "Optics and Photonics an Introduction," (Wiley & Sons, Ltd., 2000).

1. Introduction

Since the invention of optical tweezers based on a single laser beam in the eighties by Arthur Ashkin [1], it has been common notion that they exert a harmonic potential on the trapped object. This property has been utilized for performing very accurate force-distance measurements on nano-scale biological systems such as molecular motors [2, 3, 4]. With this letter we challenge this basic assumption; by an improved method we measured the optical trapping potential in a regime significantly larger than previously covered and find that the potential is not well described by a single harmonic function. This finding has implications if one wishes to exert large forces, e.g. when optically unfolding proteins or nucleic structures [5], and hence utilizes extreme parts of the potential that are typically not visited by Brownian motion at room temperature.

The first theoretical calculations of the forces exerted by optical tweezers were presented by Ashkin who in 1992 performed calculations of the optical forces in the ray optics regime [6]. His calculations have been repeated several times, e.g. in Ref. [7], where the lateral trapping efficiency versus lateral displacement is explicitly given having taken spherical aberrations into account. This ray optics calculation does not predict a linear relation between lateral force and distance, however, for small displacements the relation can be approximated as linear. For larger distances, a stiffening of the potential is predicted but was never experimentally verified.

As calculations of the forces exerted by optical tweezers are cumbersome [8], and maybe impossible in some cases, calibration is essential. The first calibrations of forces exerted by optical tweezers were done by moving the surrounding liquid with a controlled velocity, v_{stage}, with respect to the bead, and by calculating the Stokes drag on the particle, $F_{\mathrm{drag}} = 6\pi\eta a v_{\mathrm{stage}}$, where a is the radius of the bead and η the viscosity of the surrounding liquid. In this manner, the first force versus distance graph was measured and depicted in Ref.[2]. It was found to be linear over a distance of approximately 200 nm around the equilibrium point for a 0.55 μm particle. Thereafter, it was more or less established that Hooke's law could be used to describe the optical trapping force, $F_{\mathrm{trap}} = -\kappa_{\mathrm{x}} x$, where κ_{x} is the spring constant in the x direction and x is the spatial deviation of the bead from its equilibrium position. In a paper published shortly after, the linearity of the force displacement graph was used, in connection with Wang & Uhlenbeck theories of Brownian motion [9], to provide an estimate of the spring constant describing the optical trap [3]. This method is considered the most accurate calibration procedure to date; the essentials are described in e.g. Ref.[10], with more recent corrections following in [11]. It is used for various bead sizes in both the extreme Rayleigh and Mie regimes, as well as in the

#99368 - $15.00 USD Received 1 Aug 2008; revised 12 Sep 2008; accepted 15 Sep 2008; published 19 Sep 2008

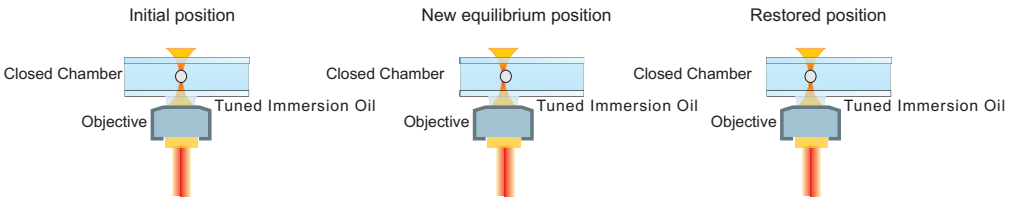

Fig. 1. Sketch of the experimental settings for performing the drag force measurements. As the stage is moved with a constant velocity (middle drawing) the bead is displaced a distance, both laterally and axially, with respect to the center of the trap.

intermediate regime.

For normal infra-red single beam laser based optical traps, the trap stiffness in the direction along the propagating laser beam, κ_z (axial direction), is lower than the trap stiffness in the directions orthogonal to the propagating laser beam, κ_x, κ_y (lateral directions) [8]. This difference in spring constant between the axial and lateral directions is due, in part, to the increased intensity gradient in the lateral directions compared to the axial direction. Therefore, when a bead escapes the optical trap it most often escapes in the axial direction. Due to the reduced axial strength of a typical optical trap, it was not previously possible to investigate the lateral potential in regions exceeding $0.6a$ [7, 12]. Considerable axial motion of a trapped bead previously lead to a theoretical overestimation of the maximum lateral trapping force [12].

The axial weakness of an optical trap is not simply due to the reduced axial focusing capabilities of ordinary lenses but is more severely caused by spherical aberrations induced in the optical pathway, resulting in an axial de-focusing [13]. Spherical aberrations are more pronounced for infra-red, laser based, optical traps that use oil immersion objectives than those formed with water immersion objectives because of the refractive index mismatch. However, by employing a recently published method [14], spherical aberrations could be almost eliminated and thus the axial trap strength significantly increased. This improved method, IM, which involves selecting an immersion media that induces spherical aberrations canceling other contributions, has produced the strongest optical trap ever reported [14].

In this letter, by using an IM optical trap, we map out the lateral optical trapping potential in regions previously unexplored by a single optical trap and find that the trapping potential is only well described by a single harmonic function within the central region. In regions extending half the bead radius the potential stiffens significantly.

2. Methods

The experimental set up was based on an inverted microscope (Leica DMIRBE) into which 1064 nm light from a Nd:YVO_4 laser (Spectra-Physics Millennia) was coupled. The laser was a TEM00 laser with a Gaussian intensity profile. The beam was first expanded (Casix 20 x) to overfill the back aperture of the objective (63 x oil Leica NA = 1.32) before it was tightly focused down to form an optical trap within the sample. The diffraction limited laser spot had a diameter of approximately 1 μm. The sample was a simple perfusion chamber containing polystyrene beads of diameter 2.1 μm with a standard deviation of 0.05 μm (Spherotech) or 2.01 μm with standard deviation 0.17 μm (Bangs). Within the uncertainties the sizes of these two beads batches are identical. The depth of the trap in the sample was maintained at 5 μm from the lower surface. The sample was mounted on a piezoelectric stage (PI-731.20) with capacitive feedback enabling precision positioning of nanometers. By driving the stage at a constant velocity, a constant drag force was applied on the bead. The stage was always driven a distance of 30 μm, at velocities between 10 μm/s and 400 μm/s depending on whether the normal method (NM),

#99368 - $15.00 USD Received 1 Aug 2008; revised 12 Sep 2008; accepted 15 Sep 2008; published 19 Sep 2008

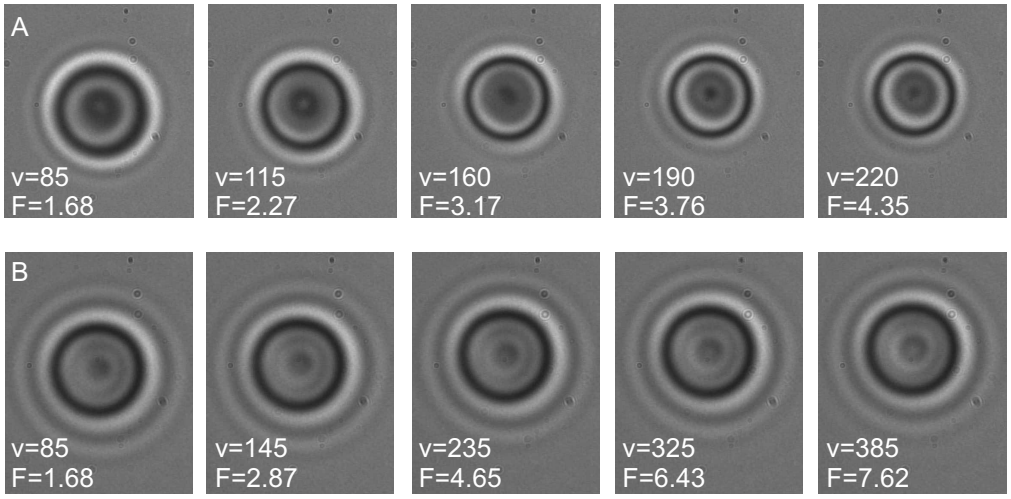

Fig. 2. CCD camera images of equilibrium bead positions as the drag force, F, is increased; v_{stage} and F are given in units if μm/second and pN, respectively. Panel A: normal setup, image diameter decreases with lateral distance. Panel B: improved setup, diameter remains constant. Both panels show the images of a 2.1μm bead in the trap

with aberrations, or the improved method (IM), without aberrations, was employed. The bead typically escaped at velocities a little over 200 μm/s for the NM and just below 400 μm/s for the IM. The stage can be moved with velocities up to 1000 μm/s. For the purposes of this investigation the minimum time for which the stage was in motion, even for the highest velocity used, was 75 ms. This time is large in comparison to the characteristic equilibrium time of the bead in the trap, 17 ms, which is given by the inverse of average measured corner frequency, f_c=60 Hz. Hence, there was no doubt that the bead reached the equilibrium position within the trap for each stage velocity. A pause of 5 seconds ensured that the bead returned to its equilibrium position at the center of the trap after stage movement. Figure 1 shows a sketch of a typical experiment as well as the sequence of motions of the piezo stage. The precise distance the bead was displaced both laterally and axially within the trap was determined by analysis of bead images collected by a CCD camera (Sony XC-ES50, 25 Hz). To increase the resolution of the system, above that the 1:1 image exiting the microscope offers, an additional lens (f=50 mm) was inserted in the image path so that the image diameter of the bead was approximately half the width of the image frame. The CCD camera was operated with the slowest possible shutter speed, 10 ms, so as to clearly identify periods where the bead was in motion by the blurring of the image. This helped to accurately determine the relative displacement between two stationary points.

Determining the lateral displacement of the bead was done by tracking the white outer ring in the bright field image of the bead, as shown in Figure 2, and counting the number of pixels its center was displaced, using a homemade Labview program. The lateral precision was $\sim$ 10 nm. The axial position of the bead with respect to the focus of the objective was found to depend linearly on the diameter of the white outer ring in the bead image; a calibration curve was performed by moving a stuck bead in known axial increments and measuring the corresponding diameter. Figure 3 shows the size of the diameter of the outer ring as a function of axial displacement. This relation serves as a calibration curve between diameter and axial displacement. The axial precision of this method was around $\sim$ 20 nm. A number of particle tracking routines are presented in literature, the method we employ is fairly similar e.g. to that

#99368 - $15.00 USD Received 1 Aug 2008; revised 12 Sep 2008; accepted 15 Sep 2008; published 19 Sep 2008

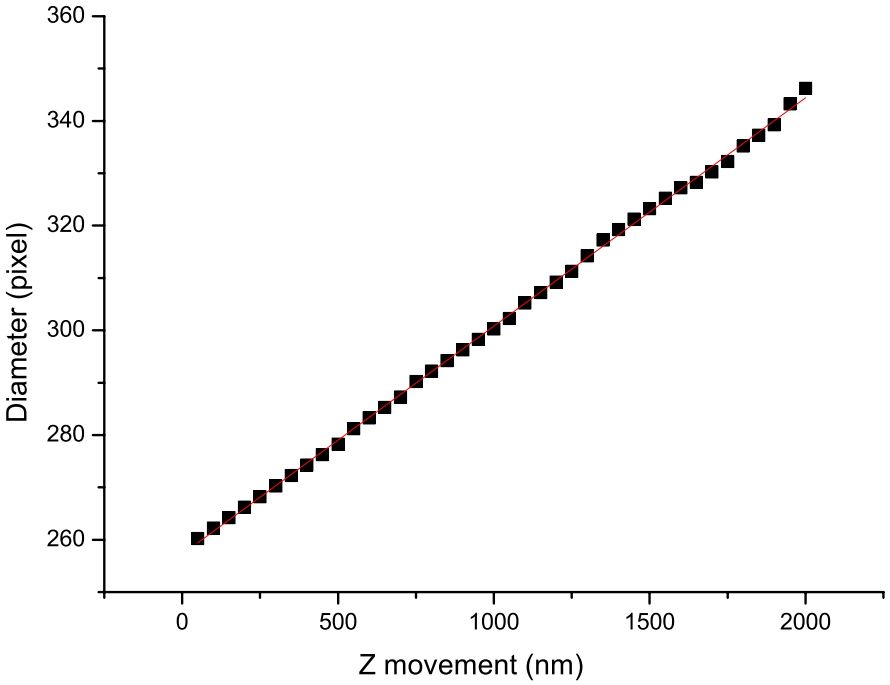

Fig. 3. Diameter of outer white ring from the image of the bead as a function of axial height, serves as a calibration curve. Curve shown is for a bead of diameter 2.1 μm.

of Ref.[15] where they followed the motion of a fluorescent bead.

Experiments were done both with the normal method, NM, and with the improved method, (IM). The NM was as described above using the immersion oil recommended by the objective manufacturer (index of refraction n=1.518). In the IM the immersion oil had n=1.54, which, following the guidelines in Ref.[14] cancels spherical aberrations at a depth of 5 μm into the sample.

3. Results and discussion

Pictures from an experiment where the relative velocity between stage and trapped bead was gradually increased in steps of 15 μm/second are shown in Figure 2. Pictures are shown both using the NM (panel A) and the IM where spherical aberrations are minimized (panel B). The picture shown for each velocity is of the stationary position after the system has equilibrated to the external force. By equating Hooke's law to Stokes drag, F_{trap} is easily found in the lateral direction. In Figure 2 the lateral motion is seen as the bead moving upwards in the picture. Using the NM (shown in Fig. 2 panel A) the bead also moves substantially in the axial direction. This is seen as a decrease in the diameter of the outer white ring. The calibration curve shown in Figure 3 was used to find the axial displacement of the bead. However, when using the IM (panel B), even by eye one could verify that the axial motion was considerably less when the bead was laterally displaced in the trap.

Figure 4 shows the axial movement in the trap as a function of the lateral displacement.

#99368 - $15.00 USD Received 1 Aug 2008; revised 12 Sep 2008; accepted 15 Sep 2008; published 19 Sep 2008

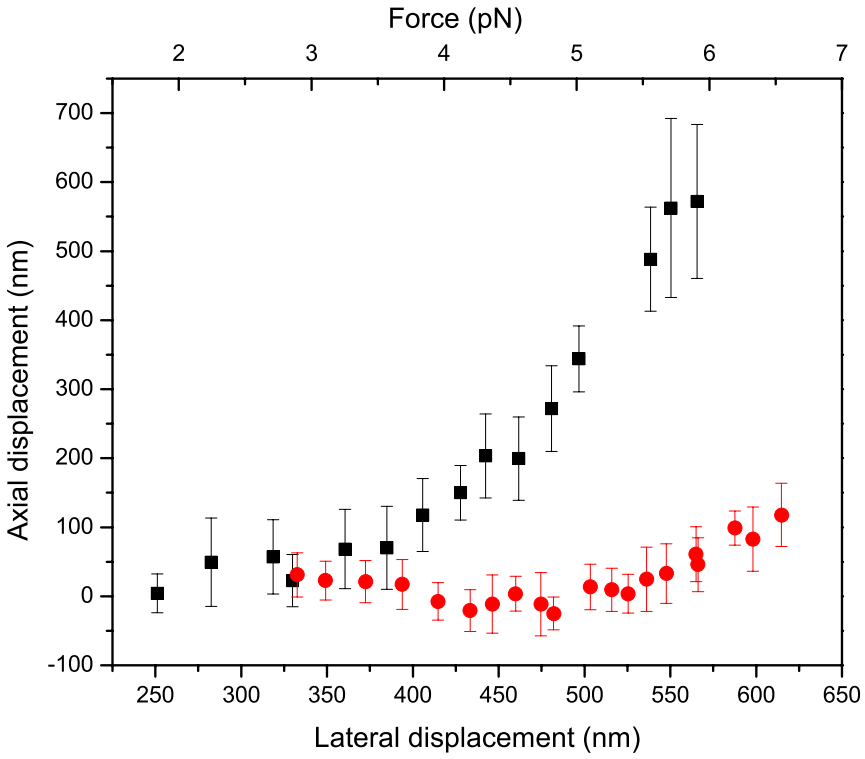

Fig. 4. The axial displacement of an optically trapped 2.01 μm bead is shown as a function of the lateral displacement. The upper axis gives the approxmiate corresponding trapping force (within 10 pct). Black squares: NM with significant spherical aberrations at the focus. Red dots: IM where spherical aberrations are eliminated. Each point on the graph represents an average of 10 data points.

The upper axis gives information about the approximate trapping force, however, as the force is related in a non-linear fashion to the lateral displacement (see Figure 5) the force values given in Figure 4 are up to 10 pct. off. The displacement values are exact. Data is shown from experiments with the NM and from experiments using the IM. Two issues are clear: i) The bead moves substantially more in the axial direction for the NM than for the IM. ii) The bead stays in the trap at considerably larger lateral forces and displacements for the IM. In other words, the bead can be forced to more extreme positions if the IM is used. Although from one experiment to the next the exact traces can look a bit different, observations i) and ii) are consistently true.

The bead escaped at a lateral displacement of 0.55*a* using the NM. This compares well with previous findings of lateral escape positions of 0.55*a* [7] and 0.6*a* [12]. The axial displacement of the bead reached 0.55*a* before escaping; this concurs with previously published experimental values of 0.45*a* [7] and 0.6-0.9*a* [12] and reiterates that the bead also moves considerably in the axial direction whilst moving laterally from the trap center. However, if the IM is used then the axial movement at the point of escape is found to be less than 0.2a, under half that observed using the NM (see Figure 4).

#99368 - $15.00 USD Received 1 Aug 2008; revised 12 Sep 2008; accepted 15 Sep 2008; published 19 Sep 2008

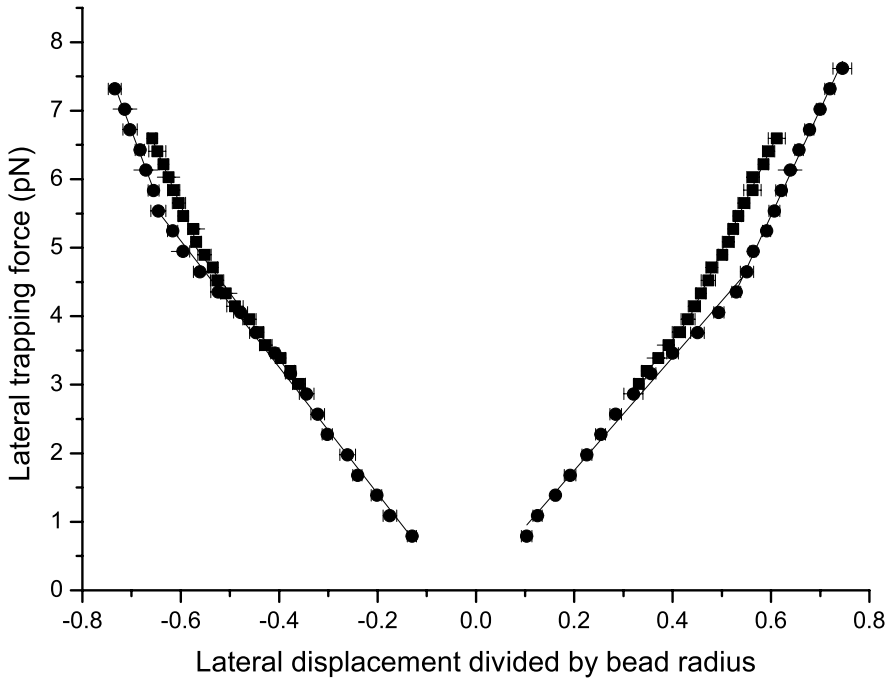

Fig. 5. Lateral trapping force as a function of lateral displacement for a 2.01 μm bead (black squares) and a 2.1 μm bead (black dots), in an optical trap. Two independent data sets are shown that were taken using the IM, minimizing spherical aberrations. Most of the error bars are smaller than the symbols. The full lines are fits to equations 1.

Figure 5 shows the lateral trapping force as a function of lateral bead displacement. The bead can be moved to a lateral position in the trap that corresponds to $0.74a$. This is a considerable improvement with respect to literature, where the furthest lateral distance experimentally explored for a single beam trap was $0.6a$ [12]. The improved method has allowed access to larger lateral regions and has enabled the investigation of the lateral trapping potential therein. Data from both negative and positive displacements are shown in order to show the symmetry of the trap. Data from two independent experiments with optical trapping of $2.01\pm0.17\mu$m and $2.1\pm0.05\mu$m beads using the IM, performed on different days are shown. Interestingly, the trapping potential is not well described by a single harmonic function. Indeed, the lower part of the potential, until $x \sim 0.55a$, is well described by a harmonic function. This is in accordance with earlier literature which has only experimentally accessed this region [2, 3, 7]. However, because the bead is forced to extreme lateral positions, with the IM, we are able to observe that the potential of the trap stiffens.

To quantify the extended optical trapping potential we have simply used two harmonic functions to describe the potential:

$$F_{\text{trap}} = \begin{cases} F_{\text{trap1}} = \kappa_1 x & \text{if } |x| < 0.55a \\ F_{\text{trap2}} = \kappa_2 x + \text{constant}, & \text{otherwise} \end{cases} \quad (1)$$

The potential of the trap as shown in Figure 5 was reasonably symmetrical. Also, the datapoints

#99368 - $15.00 USD Received 1 Aug 2008; revised 12 Sep 2008; accepted 15 Sep 2008; published 19 Sep 2008

do extrapolate to zero. Figure 5 suggests that the escape force and hence the maximum lateral trapping force are almost the same for the positive and negative sides of the potential. This was supported by an experiment where the escape velocities from positive or negative displacements were found to differ by max 5%. By fitting Equations 1 to the data shown in Figure 5 we find that $\kappa_1 = 0.0079 \pm 0.0006$pN/nm and $\kappa_2 = 0.015 \pm 0.002$pN/nm. The values given are averages of the two independent experiments and the positive and negative sides. The laser power measured at the sample was only 15 mW. This low laser power, and corresponding low spring constant, was chosen because otherwise the trap would be too strong to enable excursions to extreme positions by oscillating the stage at the obtainable frequencies.

We also performed a calibration of the trap by observing the Brownian motion of the particle [10] and tracking the bead's position by recording the back scattered light by a quadrant photodiode. A quadrant photodiode only has a linear response for bead displacements of approximately half the radius from equilibrium, hence, this method cannot be used to monitor the extreme positions which were recorded as described above. At room temperatures, the particle typically only explores the lower part of the potential depicted in Figure 5 and hence, quadrant photodiode recording of the Brownian motion can be used to find κ_1 only. By employing the equipment described in [16], the methods from [11], and the programs from [17], we found that $\kappa_1 = 0.008 \pm 0.0006$pN/nm. This is consistent with the value of κ_1 found by employing Equation 1, within the uncertainty.

We observed a pronounced stiffening of the potential as the bead visited extreme lateral positions and have found a ratio $\frac{\kappa_2}{\kappa_1} \simeq 1.8 \pm 0.2$. Many more experiments than those depicted in Figure 5 were performed; experiments were repeated over several months and because of occasional modifications to the alignment of the optical trap during this time, it is not so surprising that the exact values of κ are somewhat different from one experiment to another. However, the appearance of 2 distinct regions that diverge around $0.5a$, both of which are well fitted by a harmonic function with a stiffening of nearly a factor of 2, consistently prevailed. The experimental conditions were maintained for all experiments and beads from the same batches with low standard deviation were used to insure repeatability of the measurements.

The reason why a bead diameter of 2 μm was chosen for this study was that this is a very common size of particle to use in single molecule force measuring experiments. Maybe this particular size is often chosen because it is large enough that it easily could held by a micropipette, and that it performs substantially less Brownian motion than a smaller particle, thus making it easier to get hold of. The magnitude of the spring constant, κ_1 is known to depend on the size of the particle with respect to the wavelength of the trapping laser [8, 14, 18]. The maximum value occurs when the diameter is similar to the wavelength, for our laser which has 1064 nm in air, this corresponds to a bead diameter of 800 nm in water. By comparing the values of κ_1=0.0079 pN/nm and κ_2=0.015pN/nm taken at 15 mW at the sample to the values shown for 15 mW in Figure 3 in Ref. [14] where exactly the same setup is used, it is clear that even κ_2 is significantly smaller than the value of κ=0.055 pN/nm for a smaller particle.

To our knowledge, no theory yet predicts the type of stiffening showed in Figure 5 which was measured for an aberration free single beam optical trap. Much of the theoretical effort in predicting optical trapping potentials is based on the ray optics picture as suggested by A. Ashkin in 1992 [6]. It should be noted, that our bead size is only 2-3 times the laser wavelength and hence, it is unclear whether a ray optics approach is appropriate. Nevertheless, we compared the expression given in Ref. [6], or the nearly equivalent recent expression given in [7] to our data. However, there was neither a quantitative nor qualitative resemblance between theory and experiment. The published ray optics expressions did predict a stiffening of the potential, which we observed experimentally. However, the theoretical expression predicts a constantly increasing spring constant and not, as we observed, two distinct regions which are each fairly well

#99368 - $15.00 USD Received 1 Aug 2008; revised 12 Sep 2008; accepted 15 Sep 2008; published 19 Sep 2008

described by a single spring constant.

In an experiment involving two lasers to create two traps and the use of a third laser to follow the position of one bead, the bead had been forced to extreme positions of one of the optical traps [19]. The potential was measured and calculated using a generalized Lorenz-Mie diffraction theory for particles with diameters 3, 6, and 9 μm. The outcome was a potential which does stiffen, but it does not have two distinct linear regions. The reason for the discrepancy with our results could be that the potential in [19] is from a double trap and hence more complex than the single beam in the present study, also, the two traps are probably aberrated, and the sizes of the particles are larger. Another prediction of a stiffening potential is given in Ref. [20], where optical forces are calculated using the T-matrix method. For a 4 μm particle (with our settings), the lateral force is predicted to decrease drastically (the bead will escape) at $0.55a$ and to exhibit some gradual stiffening before this point. These predictions do not exactly correlate with our findings as the bead stays in the trap for a lateral displacement up to $0.74a$, and the functional form of the potential is different.

Presently, it is unclear what is the physical mechanism behind the observed stiffening of an aberration free single beam optical trap. One possible route to understanding the observed stiffening could be to take into account the diffraction pattern created by the illuminated circular aperture, the so-called Airy function, formulas and graphs are textbook material e.g. given in [21]. The Airy pattern has a main peak in the intensity distribution at the image plane and less intense side lobes, the intensity of the side lobes decreasing with distance to the main peak. The maximum of the side lobe closest to the main peak is located around 0.7 μm from the center of the main peak. Hence, when forcing a 2 μm bead to a lateral distance of $\sim$ 800 nm the bead will feel this side lobe as well. This might serve as a physical argument why a stiffening of the potential was observed.

Future efforts will include the investigations of the potential from different bead sizes as well as theoretical efforts and simulations in an attempt to understand the aberration free potential from a single beam optical trap here reported.

4. Conclusion

By using an improved method where spherical aberrations were eliminated, it was possible to experimentally investigate the optical trapping potential in regions significantly outwith that of previous studies. The trapping potential has, in practice, been considered harmonic and this property has formed the basis for using optical tweezers as force transducers. We find that the total lateral trapping potential is not well described by a single harmonic function. Rather, the potential is well described by two harmonic functions, the outer part of the potential being almost twice as stiff as the inner part. Optical tweezers are often used to perform accurate force measurements in regimes of hundreds of pico Newtons. At very high forces, outside the region commonly visited by thermal fluctuations, it is important to be aware of the stiffening of the potential and it would be erroneous to assume the potential to be well described by a single harmonic function. Hence, we find inadequate the commonly accepted assumption that utilising the particle Brownian motion, as described by simple Uhlenbeck theories, is sufficient to characterise the full optical trapping potential.

Acknowledgments

This work was financed by Marie Curie MP6, MEST-2004-504465 and by the Villum Kann Rasmussen Foundation through BioNET. We acknowledge discussions with A. Rohrbach.

#99368 - $15.00 USD Received 1 Aug 2008; revised 12 Sep 2008; accepted 15 Sep 2008; published 19 Sep 2008